Int. J. Electrochem. Sci., 11 **(2016)** 4399 – 4409, doi: 10.20964/2016.06.26

International Journal of
ELECTROCHEMICAL
SCIENCE
www.electrochemsci.org

Synthesis of Schiff Base Surfactants and Their Corrosion Inhibition Effect on Tubing Steel in Deep Oil Wells

Changjin Wang[1,*], *Yinpeng Li*[1] *and Wen Zhou*[2*]

[1] Department of petrochemical, Northeast Petroleum University at Qinhuangdao, No. 550 West of Hebei Rd, Haigang, Qinhuangdao, Hebei, 066004, P.R. China
[2] The Second Clinical College of Guangzhou University of Chinese Medicine (Guangdong Provincial Academy of Chinese Medical Sciences), 55 Neihuanxi Road, Guangzhou, 510006, China
[*]E-mail: changjinwang_01@126.com; xtunwen@163.com

Received: 29 February 2016 / *Accepted:* 23 March 2016 / *Published:* 4 May 2016

In this work, we synthesized a series of Schiff base surfactants using chemical route. The properties of the surfactants including critical micelle concentration, maximum surface excess, minimum surface area and surface tension were determined. Results indicate the properties of the surfactants are highly related to their chain length. The corrosion inhibition effect of the Schiff base surfactants was evaluated on deep oil well tubing steel. Electrochemical impedance spectroscopy, polarization, polarization and weight loss experiments were carried out. Surfactant molecules were well absorbed on the carbon steel surface and can be described using Langmuir adsorption isotherm. The effect of several parameters were studied and discussed.

Keywords: Schiff base surfactant; Corrosion; Deep oil well; Tubing steel; Surface tension

1. INTRODUCTION

Material loss due to the saline media corrosion on the metallic surface is an important problem in many industrial areas. In petroleum industry, corrosion of oil wells becomes a serious problem because large quantities of water (commonly known as formation water) produced along with the oil and gas as by-product. The formation water not like common waste water, many organic and inorganic compounds dissolve in the formation water due to the oil-producing process. Thus, the formation water was considered as the most corrosive liquid causing material loss in the petroleum industry due to the presence of larger amount of CO_2 and H_2S [1, 2].

In order to prevent the corrosion effect caused by the aggressive facts of the formation water, development of inhibitors become essential for the petroleum industry. For example, organic

substances which contain the electro-negative functional groups such as hydroxyl groups were commonly had good performance in corrosion inhibition when applied for many metals or alloys [3-6]. Basically, the inhibitors could adsorbed on the target surface through the functional group interaction and prevent the target material directly interact with the corrosive material, which result a low corrosion rate and consequently extending the life of the target material. Several nitrogen-based organic inhibitors were developed and showed promising performance toward corrosion inhibition. The nonionic surfactants showed high inhibition performance, which could effectively lower the critical micelle concentrations. Therefore, the nonionic surfactants were well studied for metal or alloy corrosion inhibition [7-11]. For example, Migahed et al. [12] developed a new family of Schiff base nonionic surfactants. The EIS results suggested the concentration of the Schiff base nonionic surfactant could highly affect the adsorption of the surfactant on the target material surface. Li et al. [13] studied the inhibition performance of Tween-20 on the cold rolled steel. Results showed that the inhibition efficiency increased when the concentration of Tween-20 increasing. On the other hand, the heterocyclic organic substances were also used as cationic surfactant for corrosion inhibition purpose due to the nitrogen, oxygen and sulfur atoms could act as the anchor sites for formation of inhibition layer on the target material surface [14-18].

In this study, we synthesized four Schiff base cationic compounds as surfactants for carbon steel in oil wells formation water. A series chemical and electrochemical experiments were carried out for investigating their performances.

2. EXPERIMENTS

2.1. Synthesis of the inhibitors

Ketoglutaric acid (KG) was firstly synthesized according to following procedure: esterification process was carried out using fatty alcohols: hexadecyl, octyl, octadecyl alcohols and dodecyl in the 50 mL xylene containing 0.05 g p-toluene. After reaction, the product was washed using Na_2CO_3 and separated. The organic layer of the product was then dried using $CaCl_2$. The products were denoted as KG-h, KG-o, KG-oa and KG-d. Then, the above alkyl ketoglutarate were reacted with p-aminopyridine in ethanol containing 0.05 g p-toluene sulfonic acid. The chemical reaction was underwent 12 h with reflux. The products were then filtered, washed and dried under an oven. The products were denoted as KG-Sh, KG-So, KG-Soa and KG-Sd. The above synthesized Schiff bases of alkyl ketoglutarate were then used for synthesizing Monoquaternary ammonium Schiff base–alkyl ketoglutarate. Specifically, a certain amount of the Schiff bases of alkyl ketoglutarate was reacted with 20 mL ethyl iodide in the ethanol for 6 h. After washing step, the product was recrystallized using ethanol. The final products were denoted as QKG-Sh, QKG-So, QKG-Soa and QKG-Sd.

2.2. Chemical composition of tested tubing steel and formation water

The tubing steel used in this work is X-65 type, which is a common tubing steel used in the oil wells. Table 1 shows the chemical composition of the X-65 tubing steel. Regular edged cuboids of the

tubing steel were sliced for weight loss investigation. For polarization and electrochemical studies, a small piece of the tubing steel was embedded in epoxy resin and then polished as an electrode with surface area of 1 cm^2.

Table 1. Chemical composition of X-65 tubing steel.

Element	C	Mn	Si	P	S	Ni	Cr	Mo	V	Cu	Al
Content (w/w)	0.08	1.53	0.31	0.01	0.06	0.03	0.03	0.007	0.002	0.03	0.05

The formation water was obtained from Northeast Petroleum University sample analysis lab. Table 2 shows the chemical composition of the formation water.

Table 2. Chemical composition of formation water.

Ionic type	Na^+	K^+	Ca^{2+}	Mg^{2+}	Ba^{2+}	Sr^{2+}	Cl^-	SO_4^{2-}	HCO_3^-
Concentration (ppm)	60.5	68.2	4570	1120	5.21	121	153	207	346

2.3. Weight loss measurements

Tubing steel specimens with size of 5 cm × 2 cm × 0.4 cm were used for weight loss measurements. The weight loss was collected by different immersion times of tubing steel specimens in formation water with surfactant inhibitors. Control experiment was conducted in the similar conditions without the addition of the surfactant inhibitors. The corrosion production on the tubing steel surface was washed using water. Then, the weight of the tubing steel was recorded and compared with the value of before experiment.

2.4. EDX analysis

Surface EDX analysis was performed at a JEOL 5400 SEM using tubing steel specimens as samples. Peak noise of the spectra was normalized using analytical software.

2.5. Surface tension measurements

The surface tension of the chemically synthesized surfactant inhibitors was carried out by a Tensiometer (K 100 mode).

2.6. Electrochemical characterization

A conventional three-electrodes system was used for electrochemical characterization. The tubing steel specimen was used as the working electrode. A platinum wire and a saturated calomel electrode were used as counter electrode and reference electrode, respectively. The electrochemical

measurements were conducted on a CHI 660 electrochemistry workstation and linked with Tacussel corrosion analysis software. 1 h pre-immersion of working electrode was used for establishing the steady state of the circuit potential. The polarization ability of the tubing steel was then recorded by potentiodynamic polarization curves using 1 mV/s. Electrochemical impedance spectroscopy (EIS) was used for characterizing the tubing steel in oil well formation water in the absence and presence of various surfactant inhibitors.

3. RESULTS AND DISCUSSION

3.1. Characterization of Schiff base surfactant inhibitors

The chemical composition of the synthesized Schiff base surfactant inhibitors were characterized and presented in Table 3.

Table 3. Chemical composition and structure of the synthesized Schiff base surfactant inhibitors.

Surfactant name	Structure formula	M.Wt (g/mol)	C%	H%	N%	I%
QKG-Sh	$C_{24}H_{45}O_4N_2I$	552.52	52.19	8.31	5.07	22.97
QKG-So	$C_{30}H_{57}O_4N_2I$	636.68	56.59	9.03	4.09	19.92
QKG-Soa	$C_{38}H_{72}O_4N_2I$	747.87	61.02	9.07	3.75	16.95
QKG-Sd	$C_{42}H_{79}O_4N_2I$	802.97	62.98	9.92	3.49	15.81

We studied the relationship between the surface tension and the concentration of the surfactants. Figure 1 shows the plot of the log of surfactant concentration against their surface tension. At the identical concentration, the surface tension of the surfactant was highly related to the length of the hydrophobic chain. Low depression of the surface tension was observed at the QKG-Sh due to its short hydrophobic chain. After increasing the hydrophobic chain, the surface tension of the surfactant increased by the absorption at the air/water interface due to longer hydrophobic chain. However, at high concentration stage, the surface tension of the different surfactants almost same, suggesting the various surfactants all reach to the critical micelle concentration values. Table 4 shows the surface and thermodynamic properties of the Schiff base surfactants. It can be seen that the QKG-Sd had the lowest critical micelle concentration value and the QKG-Sh had the highest critical micelle concentration value, indicating the critical micelle concentration value decreased after increasing of the hydrophobic chain. It is obvious that the lower critical micelle concentration value of the surfactant could result in high surface activity due to the existence of the azomethine and ester groups in the chemical structures [19].

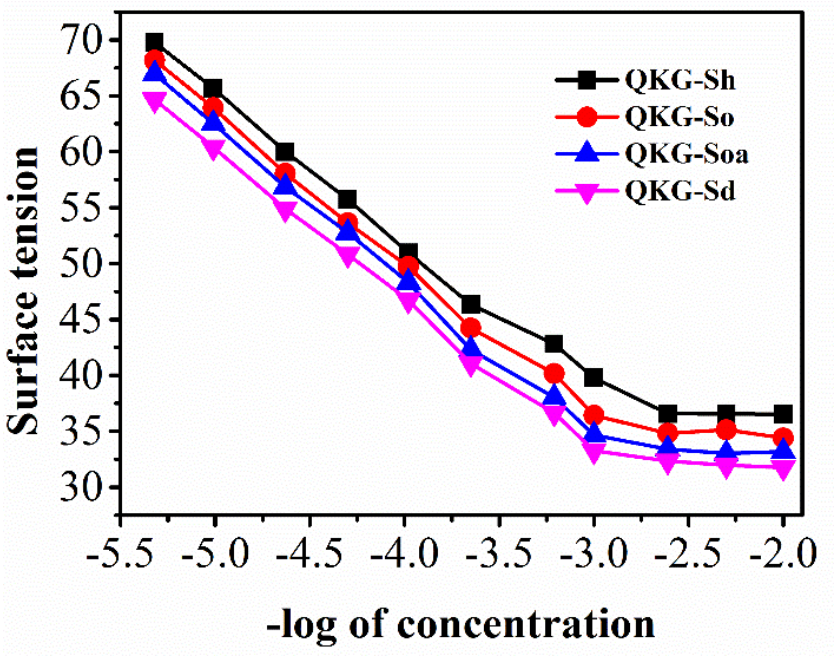

Figure 1. Relation plot of surface tension and –log concentration of the synthesized Schiff base surfactant inhibitors.

The effectiveness surface tension (π_{CMC}) and adsorption efficiency (Pc20) were determined by the surface tension of the surfactant at the critical micelle concentration and the concentration of the surfactant could lower the surface tension of the solution below 52 mN/m, respectively. The maximum surface excess value was also used for determining the surface activity and can be calculated from Gibb's adsorption equation, which increased when the hydrophobic chain length increasing. Based on above values, the highest surface activity of the surfactant can be predicted as QKG-Sd.

Standard free energies of adsorption and micellization were used for describing the thermodynamic ability of the surfactants. The standard free energies of adsorption and micellization of the surfactants at the air/water interface or in the bulk of the solution were evaluated using following equations:

$$\Delta G^0_{ads} = \Delta G_{mic} / \pi CMC / \Gamma_{\max}$$
$$\Delta G^0_{mic} = 2.303RT \log(CMC)$$

Where Γ_{max} is maximum surface excess concentration. The values of standard free energies of adsorption and micellization in synthesized surfactants were negative, suggesting the adsorption and micellization processes of the surfactant occurred spontaneously. Compare with the value number, the adsorption process of the surfactant is more dominant than that of the micellization. Due to the difference of the adsorption and micellization capability, the adsorbed molecules at the interface were highly compacted. Therefore, the water molecules cannot simply contact with molecules, which potentially provide a middle layer between the underneath material and formation water.

Table 4. Surface and thermodynamic properties of the synthesized Schiff base surfactant inhibitors.

Surfactant name	Critical micelle concentration (mM/L)	π_{CMC} (mN/m)	Pc20	Standard free energies of adsorption (kJ/mol)	Standard free energies of micellization (kJ/mol)
QKG-Sh	2.31	31.5	1.29	—32.55	—15.27
QKG-So	1.88	32.5	5.78	—33.17	—15.69
QKG-Soa	1.51	33.1	3.33	—34.21	—16.21
QKG-Sd	1.08	34.2	2.89	—35.15	—17.33

3.2. Corrosion study

Table 5. Weight loss experiment of tubing steel in formation water with or without different synthesized Schiff base surfactant inhibitors.

Inhibitor	Concentration (ppm)	Corrosion rate ($mg/cm^2/h$)	Surface coverage	Inhibition efficiency (%)
Blank	0	14.5	—	—
QKG-Sh	100	8.5	0.414	41.4
	200	8.2	0.434	43.4
	300	7.7	0.469	46.9
	500	6.8	0.531	53.1
	700	5.2	0.641	64.1
QKG-So	100	8.3	0.428	42.8
	200	8.1	0.441	44.1
	300	7.8	0.462	46.2
	500	7.2	0.503	50.3
	700	6.3	0.566	56.6
QKG-Soa	100	7.9	0.455	45.5
	200	7.2	0.503	50.3
	300	6.5	0.552	55.2
	500	5.8	0.600	60.0
	700	4.9	0.662	66.2
QKG-Sd	100	7.2	0.503	50.3
	200	6.5	0.552	55.2
	300	5.2	0.641	64.1
	500	4.1	0.717	71.7
	700	2.8	0.807	80.7

Table 5 displays the performances of different synthesized Schiff base surfactant inhibitors in the prevention of weight loss of the tubing steel samples. Inhibition efficiency and surface coverage were studied after the weight loss experiment. The corrosion rate was then calculated according to following equation: $K = \frac{W}{St}$. Where K is the corrosion rate; S is the surface coverage of the sample at time s; W is the average weight loss. The surface coverage was calculated according to following

equation: $\Theta = 1 - \frac{W_{corr}}{W^{o}_{corr}}$. Where W_{corr} and W°corr are the corrosion rate of steel samples with and without the inhibitor, respectively. The inhibition efficiency of inhibitor for the corrosion of steel was obtained by using following equation: $E = (1 - \frac{W_{corr}}{W^{o}_{corr}}) \times 100\%$. Based on the results in Table 5, we represented the result of QKG-Sd with different concentrations (Figure 2). It can be observed that the inhibition efficiency clearly enhanced when the concentration of the QKG-Sd increasing.

The open circuit potentials of the tubing steel electrode exposure in the formation water and different types of the synthesized Schiff base surfactant inhibitors with different period were studied. As shown in Figure 3A, it can be clearly seen that the open circuit potential of the tubing steel electrode tended to be more negative when exposure in the formation water at the beginning. This pheromone was consisted with other report. The main cause of this behavior is the formation of a protective film on the electrode surface by inhibitor, which could slightly change the open circuit potential towards positive [20]. Figure 3B shows the typical Tafel plots of the tubing steel electrode in the formation water with different concentrations of QKG-Sd. It can be seen that the presence of the surfactant clearly showed the inhibition of the anodic metal dissolution and the cathodic reduction reactions. Moreover, this behaviours increased along with the concentration of the QKG-Sd increasing. The cathodic and anodic Tafel slopes of the QKG-Sd at different concentrations can be determined as follow: 485 and 284 mV/dce for 100 ppm; 262 and 215 mV/dce for 200 ppm; 210 and 204 mV/dce for 300 ppm; 318 and 195 mV/dce for 500 ppm; 363 and 213 mV/dce for 700 ppm. Theshifts of Tafel slopes indicating a mixed type inhibitors were introduced [21, 22]. In addition, the corrosion density showed a decreasing when the increasing of the inhibitor concentration, indicating the introduction of the inhibitor did not change the dissolution mechanism during the retardation of the anodic metal dissolution and the cathodic reduction reactions [23-26].

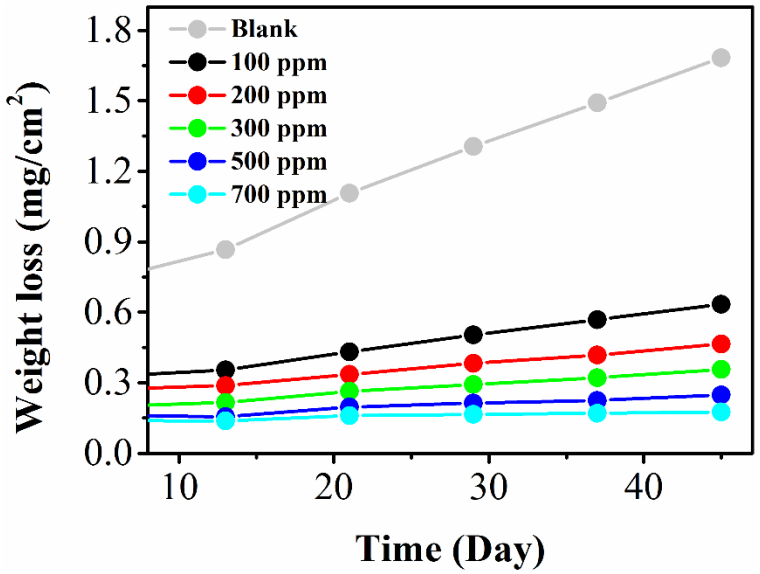

Figure 2. Weight loss profile using different concentrations of QKG-Sd as inhibitor in the formation water after 45 days.

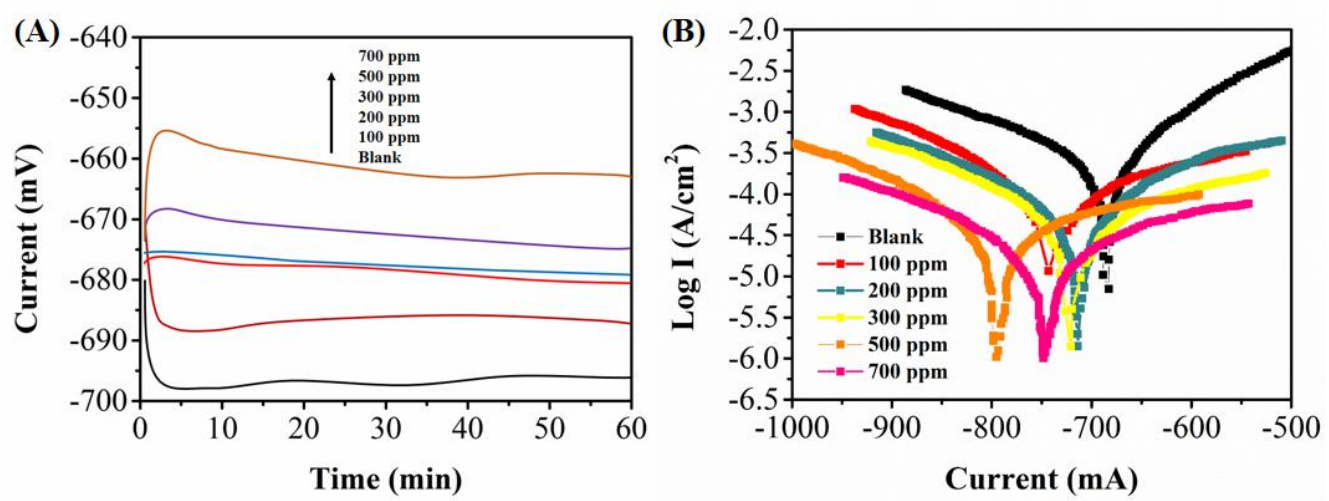

Figure 3. (A) Potential–time plots and (B) polarization curves for tubing steel in oil wells formation water in the presence of different concentrations of QKG-Sd.

Figure 4A shows the Nyquist plot of the tubing steel corrosion behavior in oil wells formation water in the presence of different concentrations of the QKG-Sd. It can be seen that the impedance response of the tubing steel electrode had a clear change after addition of different concentrations of the QKG-Sd. All curves showed an inductive line in the low frequency value and a capacitive loop at high frequency due to the frequency dispersion effect [27]. The resistance increased when the inhibition concentration increasing, suggesting the inhibitor molecules adsorbed on the tubing steel/oil wells formation water interface [28]. Figure 4B shows the Bode plots of the tubing steel corrosion behavior in oil wells formation water in the presence of different concentrations of the QKG-Sd. Results showed the slops of logZ against logf lines not equal to -1, suggesting the constant phase element verifies such condition very well [29].

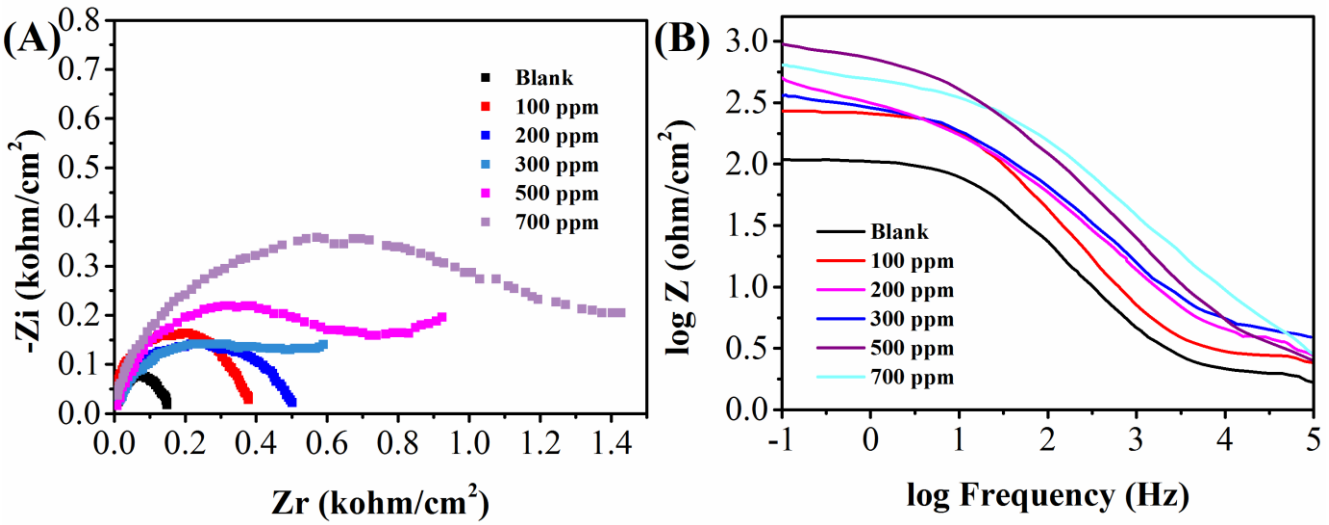

Figure 4. (A) Nyquist plots and (B) Bode plots for tubing steel electrode in oil wells formation water in the presence of different concentrations of QKG-Sd.

The electrochemical measurement confirmed the formation of a protection layer between the tubing steel surface and oil wells formation water interface. Energy dispersive analysis (EDX) was then used for analyzing the composition of the formed the protection layer. Fe signal was used for indicating the thickness of the formed protection layer. Figure 5A shows the spectrum of polished tubing steel sample without any corrosion test. Figure 5B shows the spectrum of the tubing steel immersed by oil wells formation water without any inhibitor. Many signals showed weaken due to the corrosion process. In contrast, Figure 5C shows the spectrum of the tubing steel sample immersed by oil wells formation water with 700 ppm QKG-Sd. The surface state of the tubing steel sample showed significantly improvement due to the formation of protective film as indicated by the decrease of the iron band. Therefore, the QKG-Sd could strongly attached on the tubing steel sample surface and result a high degree of inhibition efficiency [30].

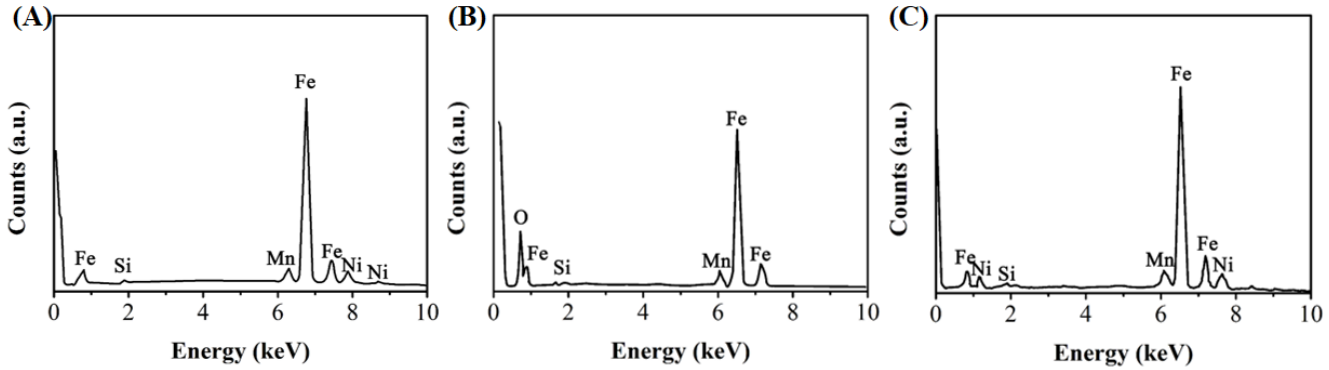

Figure 5. EDX of the tubing steel samples of (A) before immersing into formation water, (B) after immersing into formation water without any inhibitor and (C) after immersing into formation water with 700 ppm QKG-Sd.

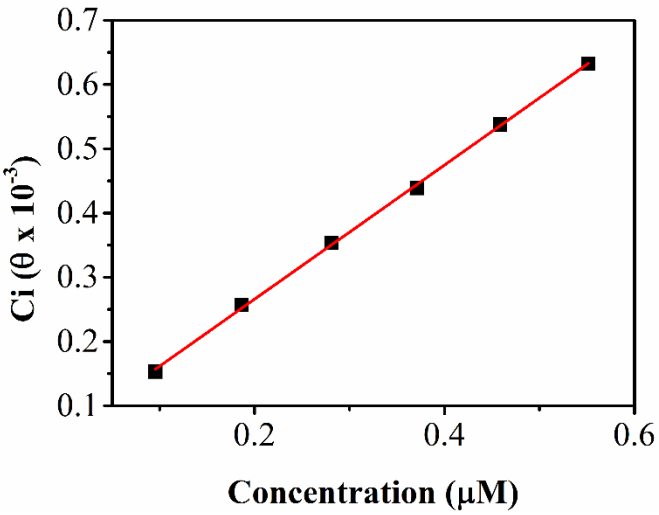

Figure 6. Langmuir adsorption isotherm model for QKG-Sd on tubing steel surface.

Based on the above experiments, the inhibition process of the inhibitor was confirmed by the formation of the inhibition layer on the tubing steel surface. We further studied the mode of the

adsorption isotherm could be used for meets the experiment results. The surface coverage was used as an indicator for explaining the adsorption isotherm. Langmuir adsorption isotherm has been found perfectly match to our experimental results. As shown in Figure 6, a straight line could be formed, suggesting the inhibition progress of the surfactant QKG-Sd is generally due to the interaction of the adsorbed surfactant molecules on tubing steel surface.

4. CONCLUSION

In this work, we synthesized four different Schiff base surfactant inhibitors. The chemical structure and properties were analyzed using different techniques. We further studied the corrosion inhibition performance of the four Schiff base surfactants in oil wells tubing steel when the presence of the formation water. The results indicated that the QKG-Sd showed best inhibition effect. The inhibition effect is also influenced by the concentrations of the QKG-Sd. Moreover, Langmuir adsorption isotherm was used for explaining the adsorption process of the adsorption process of the surfactant molecules on the tubing steel surface.

Reference

1. T. Jialin, F. Chuanhong, Y. Lin, L. Zhenglian, L. Xiaokang and F. Jian, *Chemical Engineering of Oil & Gas/Shi You Yu Tian Ran Qi Hua Gong*, 44 (2015)
2. X. Fan and K.J. Sokorai, *Postharvest Biology and Technology*, 109 (2015) 65
3. L. Fu, Y. Zheng and A. Wang, *Int. J. Electrochem. Sci*, 10 (2015) 3518
4. Y. Zheng, A. Wang, H. Lin, L. Fu and W. Cai, *RSC Advances*, 5 (2015) 15425
5. Y. Zheng, L. Fu, F. Han, A. Wang, W. Cai, J. Yu, J. Yang and F. Peng, *Green. Chem. Lett. Rew.*, 8 (2015) 59
6. L. Fu and A. Yu, *Rev. Adv. Mater. Sci*, 36 (2014) 40
7. A.M. Atta, G.A. El-Mahdy, H.A. Allohedan and S.M. El-Saeed, *Int. J. Electrochem. Sci*, 10 (2015) 8
8. A. El-Tabei and M. Hegazy, *Chemical Engineering Communications*, 202 (2015) 851
9. M. Migahed, A.A. Farag, S. Elsaed, R. Kamal and H.A. El-Bary, *Chemical Engineering Communications*, 199 (2012) 1335
10. A.A. Abd-Elaal, S.M. Tawfik and S.M. Shaban, *Appl. Surf. Sci.*, 342 (2015) 144
11. K. Mohammed, A. Hammdy, A. Abdelwahab and N. Farid, *Life Sci J*, 9 (2012) 424
12. M. Migahed, A. Farag, S. Elsaed, R. Kamal, M. Mostfa and H.A. El-Bary, *Mater. Chem. Phys.*, 125 (2011) 125
13. X. Li, S. Deng, G. Mu, H. Fu and F. Yang, *Corrosion Science*, 50 (2008) 420
14. M.A. Hegazy, A.Y. El-Etre, M. El-Shafaie and K.M. Berry, *Journal of Molecular Liquids*, 214 (2016) 347
15. A. El-Tabei, M. Hegazy, A. Bedair and M. Sadeq, *Journal of Surfactants and Detergents*, 17 (2014) 341
16. M. Hegazy, *Journal of Molecular Liquids*, 208 (2015) 227
17. S.M. Shaban, A. Saied, S.M. Tawfik, A. Abd-Elaal and I. Aiad, *Journal of Industrial and Engineering Chemistry*, 19 (2013) 2004
18. I. Zaafarany, *Int. J. Electrochem. Sci.*, 8 (2013) 9531
19. P. Sehgal, H. Doe and M.S. Bakshi, *Journal of surfactants and detergents*, 5 (2002) 123

20. E. McCafferty, *Corrosion Science*, 47 (2005) 3202
21. H. Amar, A. Tounsi, A. Makayssi, A. Derja, J. Benzakour and A. Outzourhit, *Corrosion Science*, 49 (2007) 2936
22. M. Migahed, E. Azzam and S. Morsy, *Corrosion Science*, 51 (2009) 1636
23. M. Moussa, A. El-Far and A. El-Shafei, *Mater. Chem. Phys.*, 105 (2007) 105
24. R. Solmaz, G. Kardaş, B. Yazıcı and M. Erbil, *Colloids and Surfaces A: Physicochemical and Engineering Aspects*, 312 (2008) 7
25. M. Benabdellah, R. Touzani, A. Aouniti, A. Dafali, S. El Kadiri, B. Hammouti and M. Benkaddour, *Mater. Chem. Phys.*, 105 (2007) 373
26. E. Bayol, K. Kayakırılmaz and M. Erbil, *Mater. Chem. Phys.*, 104 (2007) 74
27. M. Quraishi and J. Rawat, *Mater. Chem. Phys.*, 70 (2001) 95
28. K. Khaled, *Appl. Surf. Sci.*, 252 (2006) 4120
29. J.R. Macdonald, *Journal of electroanalytical chemistry and interfacial electrochemistry*, 223 (1987) 25
30. M.A. Amin, *Journal of applied electrochemistry*, 36 (2006) 215